This manuscript has been accepted for publication in the "Journal of Mechanical Science and Technology"

Effect of Reynolds numbers on flow past four square cylinders in an in-line square configuration for different gap spacings

Shams-Ul-Islam[1]*, Waqas Sarwar Abbasi[1], Suvash C. Saha[3], YuanTong Gu[3], Zhou Chao Ying[4]

[1] *Mathematics Department, COMSATS Institute of Information Technology Islamabad, Pakistan, 44000*

[2] *Department of Mathematics, Abdul Wali Khan University Mardan, 44000, Pakistan*

[3] *School of Chemistry, Physics and Mechanical Engineering, Queensland University of Technology, Brisbane QLD 4001, Australia*

[4] *Shenzhen Graduate School, Harbin Institute of Technology Shenzhen University Town, Shenzhen 518055, China*

Abstract

In this paper two-dimensional (2-D) numerical investigation of flow past four square cylinders in an in-line square configuration are performed using the lattice Boltzmann method. The gap spacing g=s/d is set at 1.0, 3.0 and 6.0 and Reynolds number ranging from Re=60 to 175. We observed four distinct wake patterns: (i) a steady wake pattern (Re=60 and g=1.0); (ii) a stable shielding wake pattern (80≤Re≤175 and g=1.0); (iii) a wiggling shielding wake pattern (60≤Re≤175 and g=3.0) and (iv) a vortex shedding wake pattern (60≤Re≤175 and g=6.0). At g=1.0, the Reynolds number is observed to have a strong effect on the wake patterns. It is also found that at g=1.0, the secondary cylinder interaction frequency significantly contributes for drag and lift coefficients signal. It is found that the primary vortex shedding frequency dominates the flow and the role of secondary cylinder interaction frequency almost vanish at g=6.0. It is observed that the jet between the gaps strongly influenced the wake interaction for different gap spacing and Reynolds number combination. To fully understand the wake transformations the details vorticity contour visualization, power spectra of lift coefficient signal and time signal analysis of drag and lift coefficients also presented in this paper.

Keywords: Reynolds number; Lattice Boltzmann method; Four square cylinders; In-line square configuration; Wake patterns

1. Introduction

The flow past multiple cylinders in engineering is a very important and common phenomenon, for example, heat exchanger tube arrays, overhead cables, micro-electro-mechanical systems (MEMS) and offshore structures. The flow around multiple cylinders produces some flow-induced vibration which affects the equipment life. Hence, it is important to fully understand fluid-structure interaction mechanism for quality designing of equipment. Over the past four decades, researchers mainly focused on flow past one or two cylinders [1-4]. A very few and little documentation available in the open literature for flow past more than two cylinders because of some important engineering parameters such as gap spacing (g=s/d) and Reynolds number ($Re=U_\infty d/\nu$), where s is the surface-to-surface distance between four cylinders, d is the size of the cylinder, U_∞ is the uniform inflow velocity, and ν is the fluid kinematic viscosity that could affect the wake patterns. The two cylinder arrangement categorized by Zdravkovich [5] into three types: (i) tandem, (ii) side-by-side and (iii) staggered arrangements. Compared to experimental measurements the numerical study shows more in-depth details and their effects on the wake patterns transformation and force statistics such as mean drag coefficients (Cdmean), Strouhal number ($St=f_s d/U_\infty$), root-mean-square values of drag (Cdrms) and lift (Clrms) coefficients, where f_s is the vortex shedding frequency determined from the power spectrum analysis of lift coefficients using the Fast Fourier Transform (FFT). Furthermore, numerically we can easily analyze the drag ($Cd=2F_D/\rho U^2_\infty d$) and lift ($Cl=2F_L/\rho U^2_\infty d$) coefficients, where F_D and F_L are the force components in the streamwise and transverse directions; respectively.

It is also important to mention here that the flow exhibits a number of differences behind square cylinders compared to circular cylinders. Firstly, there is an interaction between the two inner shear layers even at large gap spacing because of the angle of separation shear layer. Secondly, the diverging and converging compared to square cylinders implies a smaller pressure loss for flow past two circular cylinders. For more details readers are refer to Alam *et al.* [6]. Experimentally they observed single-body sub-regime ($g \leq 1.02$) and the single-body-like sub-regime ($1.02 < g < 1.3$), biased flow between cylinders (g = 1.3-2.2), transition regime (g = 2.2-3.0) and coupled vortex-shedding regime (g = 3.0-4.6) at Re = 47000 using quite different techniques, including load cell, hot wires, laser-induced fluorescence flow visualization and particle imaging velocimetry.

*Corresponding author. Tel.: +92-3139840066
E-mail address: islam_shams@comsats.edu.pk

Kang [3] numerically examined flow past two side-by-side circular cylinders at $g < 5$ and low Reynolds numbers ($40 \leq Re \leq 160$) using the immersed boundary method. The author observed antiphase-synchronized ($g \geq 2$), in-phase-synchronized ($g \geq 1.5$), flip-flopping ($0.4 \leq g \leq 1.5$), single bluff-body ($g \leq 0.4$), deflected ($50 \leq Re \leq 110$ and $0.2 \leq g \leq 1$), and steady wake patterns ($Re \leq 40$ and $g \geq 0.5$). The author also observed that the wake patterns strongly depend both on the gap spacing (g) and Reynolds number, but the gap spacing shows more effect as compared to the Reynolds number.

Agrawal *et al.* [4] numerically investigated the effect of gap spacing at $g = 0.7$ and 2.5 and $Re = 73$ for flow past two side-by-side square cylinders using the lattice Boltzmann method (LBM). They observed flip-flop ($g = 0.7$) and synchronized ($g = 2.5$) wake patterns. They further investigated that these wake patterns strongly depended on the jet between the cylinders with the adjoining wakes and the strength of this interaction strongly depended on the gap spacing.

Experimental studies have been carried out for flow past four circular cylinders in an in-line square configuration. Sayers [7] experimentally measured the drag and lift coefficient using open-jet wind tunnel at g ranging from 1.1 to 5.0 and Re=30000 for four equally spaced cylinders. The author compared the results with a group of three cylinders and found similar data behavior. Sayers [8] experimentally measured the vortex shedding frequencies (St) for three and four equispaced circular cylinders using the same open-jet wind tunnel technique. The author found that at $g \geq 4.0$ and Re=30000, the Strouhal numbers is equal to those for flow past single isolated circular cylinder. Furthermore, the author observed that at $g < 4.0$ and Re=30000, the Strouhal numbers showed sudden changes in value and varied across the wake. Lam and Lo [9] experimentally conducted different kinds of wake patterns and there corresponding Strouhal number for four circular cylinders at Re=2100, g ranging from 1.28 to 5.96 and blockage ratio ($\beta = H/d = 21.3$). They observed three different kinds of wake patterns: (i) the generated shear layers of the upstream cylinder is shielded the downstream cylinder, (ii) the generated free shear layers reattached onto the downstream cylinder produced by the upstream cylinder and (iii) the upstream cylinder shed vortices and is impinged the downstream cylinder. They also observed that due to wide wake of low shedding frequency and narrow wake of high frequency there exist a bistable flow feature. Lam and Fang [10] experimentally studied force coefficients and flow interference effects of four cylinders at g=1.26-5.80, $\beta = 28.4$ and Re=12800. They noticed that the critical gap spacing is different compared to two and three cylinders and to be g=2.7. Several other researchers (Lam *et al.* [11-14]) also confirmed different kinds of wake patterns using quite different experimental techniques such as digital particle imaging velocimetry (DPIV) and laser induced fluorescence (LIF) flow visualization technique for flow past four circular cylinders in an in-line square configuration.

In the last two decades for solving complicated engineering problems for flow past single and multiple cylinders computational fluid dynamics (CFD) has become a powerful tool. Compared to experimental studies numerical investigation of flow past four circular cylinders in an in-line square configuration is relatively less. Farrant *et al.* [15] numerically examined the in-phase and anti-phase vortex shedding and synchronized vortex shedding at Re=200 using the cell boundary element method. Lam *et al.* [16] also observed similar flow characteristics using surface vorticity method at g=1.5 and Re=1300. They observed such well-known characteristics in this complicated flow which are mostly observed for two cylinders [3, 4]. Lam *et al.* [17] numerically examined flow around four circular cylinders in an in-line square configuration using a finite-volume method at Re=100 and 200, $\beta = 16$ and g ranging from 1.6 to 5.0. They noticed three distinct wake patterns: (i) a stable shielding wake pattern, (ii) a wiggling shielding wake pattern and (iii) a vortex shedding wake pattern. They further noticed jump change in engineering parameters such as Cdmean, Cdrms and Clrms when the flow transformation occurs. Readers are also referred to some other existing numerical investigations [18-20] for flow past four circular cylinders in an in-line square configuration.

The motivation of present numerical investigation is of importance in engineering applications. To get reliable knowledge of important parameters, such as vortex shedding frequency, wake patterns, and drag and lift coefficients, understanding of basic fluid mechanics in case of multiple cylinders is very important for designing. In the present numerical study, for complex multi-cylinder configurations, more than two cylinders are needed; therefore, we use four square cylinders in an in-line square configuration. It should be mentioned that there is some experimental [7-14] and numerical [15-20] study on flow past four circular cylinders in an in-line square configuration in the open literature. To the best of author's knowledge, no experimental and numerical study available for gap spacing and Reynolds number effect for flow past four square cylinders in an in-line square configuration. Furthermore, only one numerical study available for four square cylinders in an in-line rectangular configuration at fixed Reynolds number (Re=100). Islam *et al.* [21] numerically examined the effect of gap spacing (g = 0.5-10) for flow around four square cylinders in an in-line rectangu-

lar configuration using the LBM at Re = 100. They observed that different wake patterns (single square cylinder, stable shielding flow, wiggling shielding flow and a vortex shedding flow) strongly depended on the gap spacing.

Furthermore, there are two more important concepts: (i) variation in the wake size [2, 22] and (ii) merging of jet flows [23, 24] were not considered for four circular cylinders case. In the present numerical work we will discuss in details and argue that the jet flow between the cylinders for different gap spacings and Reynolds numbers substantially affect the wake interaction dynamics.

The organization of the present paper is as follows. Section 2 consists of computational domain, LBM, boundary conditions, grid independence and code validation. The time history analysis of drag and lift coefficients signal, power spectrum analysis of lift coefficient signal, instantaneous vorticity contour visualization, and analysis of important engineering parameters is presented in four subsections in section 3. Finally, in section 4 some conclusions are drawn.

2. Problem description and code validation study

In this study, the computational domain in the longitudinal and transverse direction varies for different g (see Table. 1). The four cylinders are located at Lu=5d from the inlet location, and are Ld=18d from the outlet position (see Fig. 1). H is the height of the computational domain. In Fig. 1, c_1, c_2, c_3 and c_4 are first, second, third and fourth cylinder, respectively. It was tested that the present computational results are not dependent on the *x*-location of the four cylinders (Table. 2). It is important to mention here that in this study the four cylinders are actually present in the computational domain, and by adopting periodic boundary conditions the results were extended to all four cylinders [32].

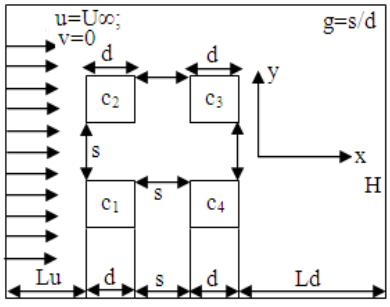

Fig. 1. Schematic configuration of four square cylinders in an in-line square configuration.

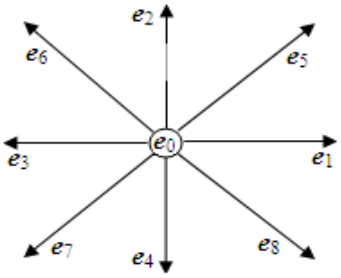

Fig. 2. Two-dimensional nine-velocity lattice (D2Q9) model.

Table 1. Selected gap spacings.

Re	g	(Lu×Ld)×H
60≤Re≤175	1.0	521×521
60≤Re≤175	3.0	561×561
60≤Re≤175	6.0	621×621

2.1 Lattice Boltzmann Method (LBM)

In this study a 2-D numerical code was developed for flow past four square cylinders in an in-line square configuration at g=1.0, 3.0 and 6.0 and Reynolds numbers ranging from 60 to 175. In LBM at each computational time the eight moving particles collide and change their velocity direction. However, during particles collision the net mass and momentum are conserved. Therefore, streaming and collisions of particles are the two basic steps of LBM. Several interesting applications regarding to LBM has found like two-phase flows and flows through porous media, readers can see Chen and Doolen [26] for a review of its applications and technique and a book [27]. Due to easy parallelization and an ease of introducing obstacles in the flow field are some of the advantages of LBM. On the basis of above mentioned advantages LBM is suitable for the present numerical study.

A brief overview of the LBM is presented in this section. A D2Q9 (where D is the space dimensions and Q is the number of particles) two-dimensional is adopted in this study. In D2Q9 model, each computational node comprises a rest particle and eight moving particles (see Fig. 2). The evolution density equation is given by

$$g_i(\boldsymbol{x}+\boldsymbol{e}_i,t+1)= g_i(\boldsymbol{x},t)-[\, g_i(\boldsymbol{x},t)- g_i^{eq}(\boldsymbol{x},t)]/\tau, \quad (1)$$

where g_i is the particle distribution function, g_i^{eq} is the corresponding equilibrium distribution function, $\boldsymbol{e}_i$ are the velocity directions, t is the dimensionless time, $\boldsymbol{x}$ is the position of particles, and τ is single relaxation time.

The equilibrium distribution function is computed as below

$$g_i^{eq}=\rho w_i(1+3(\boldsymbol{e}_i.\boldsymbol{u})+4.5(\boldsymbol{e}_i.\boldsymbol{u})^2-1.5\boldsymbol{u}^2), \quad (2)$$

where at each computational node $\boldsymbol{u}$ is the instantaneous velocity, ρ is the fluid velocity, and w_i are the corresponding weighting functions (w_i = 4/9 for i = 0, w_i = 1/9 for i = 1, 2, 3, 4 and w_i = 1/36 for i = 5, 6, 7, 8). The single re-

laxation time is related to the kinematic viscosity of the fluid

$$\nu=(2\tau-1)/6. \quad (3)$$

Using Bhatnagar-Groos-Krook (BGK) collision operator [28] Eq.(1) is solved in two steps of collision and streaming. During the collision step, the particles readjust their states and the total mass and momentum is conserved at each computational node. In the streaming step, the particles along their velocity directions move to the nearest computational node. Mathematically, the collision (Eq. (4)) and streaming (Eq. (5)) can be expressed as

$$g_i^*(\boldsymbol{x},t)= g_i(\boldsymbol{x},t)-[\, g_i(\boldsymbol{x},t)- g_i^{eq}(\boldsymbol{x},t)]/\tau, \quad (4)$$

where g_i^* is an intermediate particle distribution function, and

$$g_i(\boldsymbol{x}+\boldsymbol{e}_i,t+1)= g_i^*(\boldsymbol{x},t). \quad (5)$$

The inlet, outlet, walls and cylinder surface boundary conditions are applied after the streaming step (Eq. (5)), and iteratively the entire process is solved. The following equations (Eqs. (6) and (7)) are used to calculate the density and velocity at each computational node:

$$\rho=\sum_i g_i, \quad (6)$$

$$\rho\boldsymbol{u}=\sum_i g_i\boldsymbol{e}_i. \quad (7)$$

In LBM the pressure is calculated using equation of state

$$P= \rho c_s^2. \quad (8)$$

where $c_s^2 = 1/3$ (c_s is the speed of sound) in the present model.

Frisch *et al.* [29] mathematically shown that the solution of Eq. (1) using the collision and streaming steps in LBM is equivalent to solving the Navier-Stokes equations provided that there is sufficient amount of symmetry for the LBM lattices. Furthermore, LBM has a second-order numerical accuracy [26]. Breuer *et al.* [30] compared the LBM with the finite-volume method for flow past a single square cylinder using different blockage ratios and Reynolds numbers. They observed satisfactory agreement between the two computational methods.

2.2 Boundary conditions and grid independence study

The flow behind four square cylinders in an in-line square configuration as presented in Fig. 1. At the entrance, a uniform inflow velocity ($\boldsymbol{u} = U_\infty$, $\boldsymbol{v} = 0$) along x-direction is applied. At the outlet boundary, the convective ($\partial\boldsymbol{u}/\partial x = \partial\boldsymbol{v}/\partial x = 0$) boundary conditions for all flow variables are applied [30]:

$$\partial_t\varphi+ U_\infty\partial_x\varphi=0, \quad (9)$$

where $\varphi=\rho, \rho\boldsymbol{u}, \rho\boldsymbol{v}$.

No-slip ($\boldsymbol{u} = \boldsymbol{v} = 0$) boundary conditions at the solid surfaces are applied [30]. The hydrodynamic force on the square cylinders adopted using the momentum-exchange method [31]. Periodic boundary conditions are applied on the lower and upper walls of the computational domain [32]. All the computations are carried out on a Dawning Parallel Computer TC4000.

Computations are normally terminated when the following convergence criteria is satisfied

$$\frac{\sqrt{\sum_{l,m}[u_{l,m}^{(k+1)}-u_{l,m}^{(k)}]^2}}{\sqrt{\sum_{l,m}[u_{l,m}^{(k+1)}]^2}} \le 1\times10^{-6}$$

A grid dependence study is carried out for different combinations of Lu and Ld at g = 3.0d. The computational results of the Cdmean obtained for different cases are summarized in Table 2. In Table 2, the discrepancies between the results in percentage are also shown. It is noted that at Lu = 5.0d and Ld = 18.0d the Cdmean shows good results compared to other combinations. In other chosen combinations such as Ld= 22.0d we also need more grid points. In previous studies Breuer *et al.* [30] already mentioned that a high resolution is required only at large Reynolds numbers. All the numerical results in this study based on Lu = 5.0d and Ld = 18.0d.

Table 2. Grid independence study at Re=150.

Lu	Ld	g	Cdmean1	Cdmean2	Cdmean3	Cdmean4
4.0d	18.0d	3.0d	1.6912	1.6912	1.3741	1.3741
			(0.54%)	(0.54%)	(0.85%)	(0.85%)
5.0d	18.0d	3.0d	1.6821	1.6821	1.3624	1.3624
			(0.125%)	(0.12%)	(0.19%)	(0.19%)
6.0d	18.0d	3.0d	1.6801	1.6801	1.3598	1.3598
			(1.24%)	(1.24%)	(1.63%)	(1.63%)
5.0d	15.0d	3.0d	1.7012	1.7012	1.3823	1.3823
			(1.26%)	(1.26%)	(1.61%)	(1.61%)
5.0d	22.0d	3.0d	1.6798	1.6798	1.3601	1.3601

It is important to state here that in this study in terms of vorticity contours the solid line represent the positive vorticity and the dotted line represent negative vorticity. Furthermore, for time signal analysis of drag and lift coefficients the solid, dashed, dotted and dashed-dotted line represents the first, second, third and fourth cylinder, respectively.

2.3 Code validation study

In this sub-section, the unsteady flow past a single square cylinder at Reynolds numbers ranging from 60 to 175 is simulated to use as a reference for further numerical investigation of flow past four square cylinders. A computational domain of 35.0d×10.0d is used for simulation and the upstream distance from the inlet position is located at 6.0d from the surface of the cylinder and the outlet boundary 28.0d downstream, the lower and upper walls are located at 10.0d. Computational results of

Cdmean and Clrms, are compared with existing experimental measurements of Okajima [33], Davis and Moore [34] and Dutta *et al.* [35], and numerical data of Gera *et al.* [36] and Malekzadeh and Sohankar [37] (see Fig. 3 (a, b)). It is seen that the present calculation and other existing numerical data for the Cdmean at Re = 100 is either above or below compared to experimental data of Okajima [33], Davis and Moore [34] and Dutta *et al.* [35]. It is observed that the present calculation for Cdmean (Fig. 3(a)) and Clrms (Fig. 3(b)) at Re =60 to 175 is very close to the numerical results of Gera *et al.* [36] and Malekzadeh and Sohankar [37]. The general trend from all of the numerical studies is similar, and the present result agrees well with that from Gera *et al*. [36] and Malekzadeh and Sohankar [37].

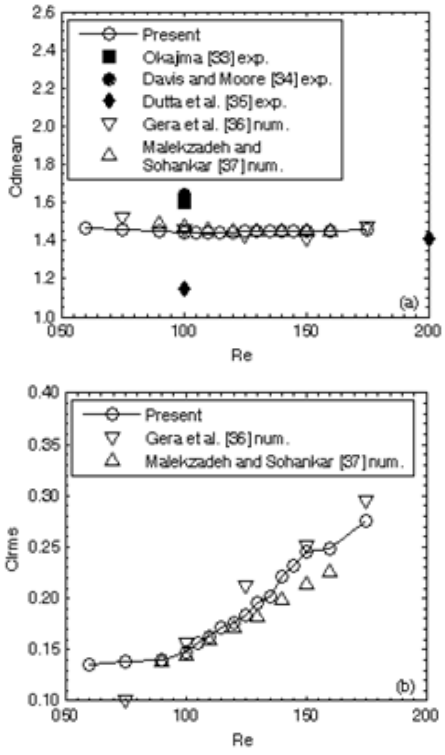

Fig. 3. Comparison of present and available experimental [33-35] and numerical [36, 37] results of mean drag coefficient and root-mean-square value of lift coefficient as a function of Reynolds number (a) mean drag coefficients and (b) root-mean-square value of lift coefficient.

For the second validation case the flow past four square cylinders at g = 5.0 and Re=200 is presented in this subsection. Figure 4(a, b) show the structure comparison between four square and circular cylinders at Re = 200 and g=5.0d. The qualitative comparison shows that the present numerical code is suitable for such complicated flow configuration.

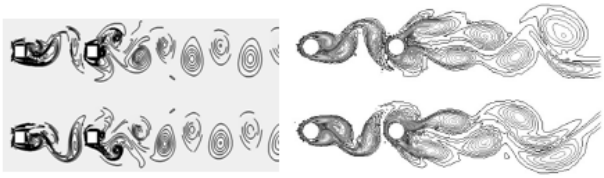

(a) Square cylinders. (b) Circular cylinders.

Fig. 4. Instantaneous vorticity contours visualization at g=5.0d and Re=200. (a) Present and (b) Lam *et al.* [17].

3. Results and discussion

After verifying the present numerical Lattice Boltzmann Method, we have systematically conducted numerical simulations by varying the Reynolds numbers for flow past four square cylinders using small, intermediate and large gap spacing between the cylinders (see Table 1). We assign the names to wake patterns on the basis of wake interactions, jet flows, power spectrum analysis of lift coefficients and time history analysis of drag and lift coefficients. We mainly concentrate on primary and secondary cylinder interaction frequencies when the wake pattern transformation occurs. Kumar *et al.* [23] numerically examined for the first time the secondary cylinder interaction frequency to the widening and narrowing of the wakes, and in this numerical investigation we are hereby examining the effect of Reynolds number for three chosen gap spacing for flow past four square cylinders in an in-line square configuration from a same viewpoint. To know more in-depth about this practicable engineering problem the distortion of shed vortices and merging of jets called wake interaction mechanism proposed by Kumar *et al.* [23] also explored in this numerical study. We found that in case of multiple cylinders more important and interesting kind of wake patterns occur. The wake patterns in this work demarcated based on power spectrum analysis of lift coefficients, time signal analysis of drag and lift coefficients and vorticity contour visualization, at g= 1.0, 3.0 and 6.0 and $60 \leq Re \leq 175$. It is also important to state here that in this numerical study we present some selected cases and those cases that they have similar characteristics in terms of power spectrum analysis, time signal analysis and vorticity contours are not shown.

3.1 Wake pattern analysis

At g=1.0, for various Reynolds numbers the vorticity contours visualization are shown in Fig. 5(a-f). It is found that at g=1.0 and Re=60 no vortices generated between and behind the cylinders (see Fig. 5(a)). The shear layers separated from the upstream cylinders (c_1 and c_2) reattached to downstream cylinders (c_3 and c_4). Such kind of wake pattern is called ‘steady wake pattern’. In Figs. 5(b-

f), from the upstream cylinders free shear layers between two inner sides quickly reattach onto the downstream cylinders surfaces. Furthermore, there is no reattachment between the downstream cylinder surfaces and the outside free shear layers from the upstream cylinders. As a result the downstream cylinders are completely engulfed. We not found any significant wiggling between the inner and outer side free shear layers. It is observed that during the whole computational process the wake pattern is almost steady. On the basis of above observations such kind of wake pattern is called the 'stable shielding wake pattern'. Lam *et al.* [17] observed similar wake pattern for flow past four circular cylinders in an in-line square configuration at Re=100 and 200 and g=1.6 and Re=100 and g=2.5.

Furthermore, it is found that the shed vortices merge behind the downstream cylinders at small downstream distance for all chosen Reynolds numbers (see Figs. 5(b-f)) except Re=60. The shed vortices behind the downstream cylinders either narrower or wider compared to isolated wake. One can clearly see the complete chaotic flow structure behind the downstream cylinders as they move downstream and there is no relation between the shed vortices. At higher Reynolds numbers behind the downstream cylinders the merging of vortices becomes stronger and stronger at Re=150 (Fig. 5(e)) and Re=175 (Fig. 5(f)). These figures clearly show the effect of jet flow between the cylinders. It is observed that the incoming jet mass laterally spread and as a result the adjoining wakes deflects in various directions behind the downstream cylinders. It is observed that at g=1.0 the jet strongly spread laterally behind the downstream cylinders because of larger acceleration of the fluid. Agrawal *et al.* [4] also found that the wake patterns strongly depended on the jet between the cylinders with the adjoining wakes for two side-by-side square cylinders using LBM at Re=73 and g=0.7 and 2.5. Kumar *et al.* [23] and Chatterjee *et al.* [24] also observed the importance and effects of merging of jets for flow past row of square cylinders.

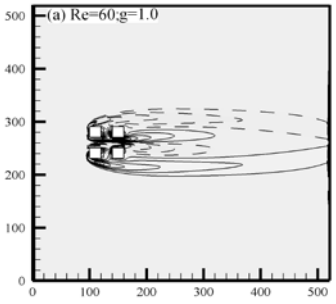

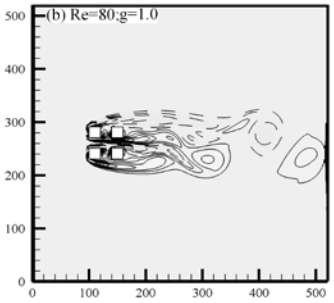

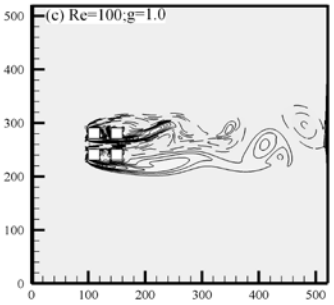

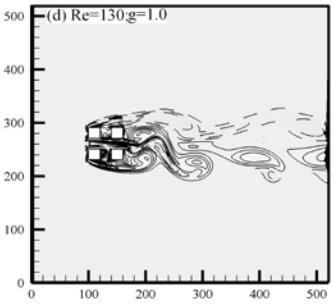

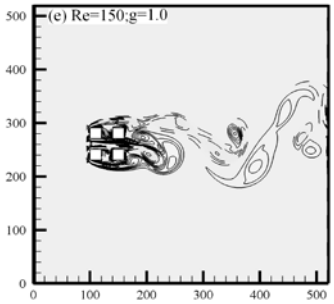

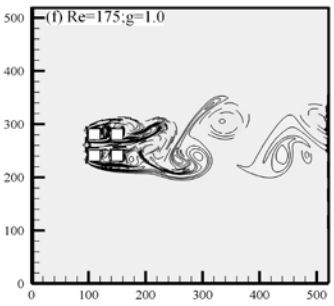

Fig. 5. Instantaneous vorticity contours for different Reynolds numbers (a) Re=60, (b) Re=80, (c) Re=100, (d) Re=130, (e) Re=150 and (f) Re=175 at g=1.0.

In Figs. 6(a-d), the outer side free shear layers do not reattach to the downstream cylinders while the two inner side free shear layers reattach. Furthermore, near the downstream cylinders alternately wiggling observed because of outer side free shear layers. This kind of flow structure is called the 'wiggling shielding wake pattern'. Lam *et al.* [17] numerically observed such kind of wake pattern for flow past four circular cylinders in an in-line square configuration using the finite-volume method at Re=100 and g=3.5 and 4.0 and Re=200 and g=2.5. The wiggling and generated vortices behind the downstream cylinders can be clearly seen when the Reynolds number increases (see Fig. 6(c-d)). It is also found that after wiggling near the downstream the shed vortices independently moves. It is observed that at higher Reynolds number the shed vortices attain the same width and size, rather than becoming short or longer. It is found that the generated vortices between the upstream and downstream cylinders either in-phase (Re=60, 80, 90, 100, 130 and 150) or anti-phase (Re=110, 120, 160 and 175) when the Reynolds number changes from Re=60 to 175.

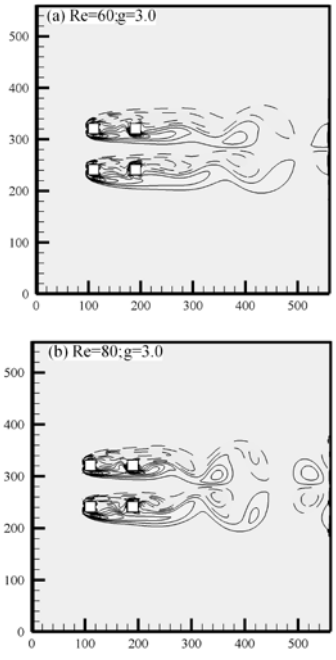

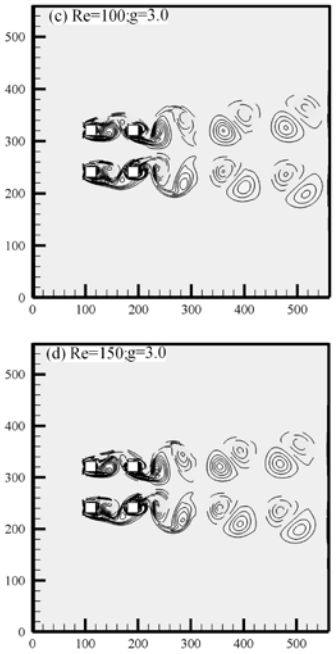

Fig. 6. Vorticity contours visualization for various Reynolds numbers (a) Re=60, (b) Re=80, (c) Re=100 and (d) Re=150 at g=3.0.

The vorticity contour visualization for different Reynolds numbers at g=6.0 are shown in Figs. 7(a-d). It is observed that between cylinders 1and 2 and 3 and 4 there is a large scale recirculation region. The roll up into mature vortices because of free shear layers observed on the upstream cylinders and then shows impinge behavior on the downstream cylinders. This kind of flow structure is defined as 'vortex shedding wake pattern'. In this study we observed in-phase (Re=120, 150 and 160) and anti-phase (Re=60, 80, 90, 100, 110, 130 and 175) vortex shedding wake patterns. This observation is in consistent with Farrant *et al.* [15] and Lam *et al.* [17]. Farrant *et al.* [15] found in-phase and anti-phase vortex shedding wake patterns using the cell boundary element method for Re=200. Lam *et al.* [17] observed in-phase and anti-phase vortex shedding wake patterns for flow past four circular cylinders in an in-line square configuration at Re=100 and g=5.0 and Re=200 and g=3.5 and 4.0 numerically. We further observed that in in-phase and anti-phase vortex shedding wake patterns the surrounding shed vortices behind the upstream and downstream cylinders not affect each one and moves almost parallel in the streamwise direction and no distortion and merging of shed vortices observed (see Fig. 7(a-d)). This ensures that the strength is almost equal of the adjoining vortices.

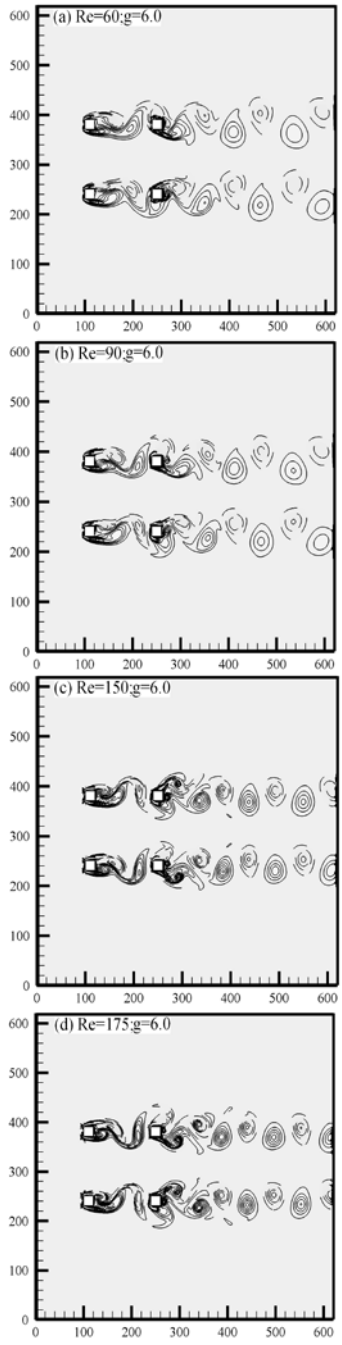

Fig. 7. Instantaneous vorticity contours for different Reynolds numbers (a) Re=60, (b) Re=90, (c) Re=150 and (d) Re=175 at g=6.0.

The shed vortices almost remain distinct and moves forward without any lateral spread and distortion. For such kind of wake patterns the wake interaction is too weak because of relatively large gap spacing between the upstream and downstream cylinders. This ensures that at relatively large gap spacing the in-phase and anti-phase vortex shedding wake patterns are predominant in case of four square cylinders in an in-line square configuration. Kumar *et al.* [23] observed similar findings for flow past row of square cylinders. Williamson [25] experimentally observed anti-phase vortex shedding wake pattern for two side-by-side circular cylinders for Re=100 and g=3.0.

3.2 Time signal analysis of drag and lift force coefficients

It is important to state here that when the amplitude of upstream and downstream cylinders are same, then we can see only the solid line and dash-dotted line in drag and lift coefficients figures in this sub-section. At g=1.0 and Re=60, the time signal analysis of drag and lift coefficients shows steady behavior (see Fig. 8 (a, b)). No modulation and periodic behavior observed for both drag and lift coefficients. Furthermore, at g=1.0 and Re=80, small modulation exists for drag and lift coefficients (see Fig. 9 (a, b)). The existence of a secondary cylinder interaction frequencies and its important contribution in the time signal analysis of drag and lift coefficients is an important property of stable shielding wake pattern. The time history analysis for some selected Reynolds numbers shown in Fig. 9(a, b) to 12 (a, b) confirm that the flow behaves like stable shielding. It is found that the time signal analysis of drag and lift coefficients from Re=80 to 175 for stable shielding wake pattern ensure that the corresponding time periods of cycles are not same (see Figs. 9 (a, b)-12 (a, b)). Chatterjee *et al.* [25] observed similar time signal analysis at small gap spacing for flow past row of square cylinders.

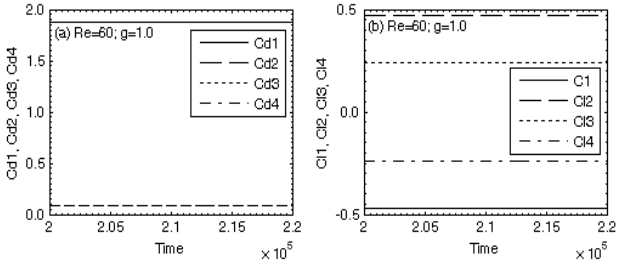

Fig. 8. Time signal analysis of drag and lift coefficients.

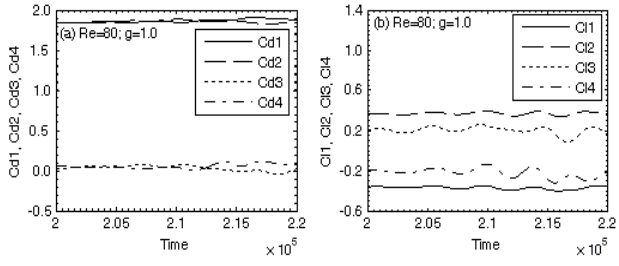

Fig. 9. Time history analysis of drag and lift coefficients.

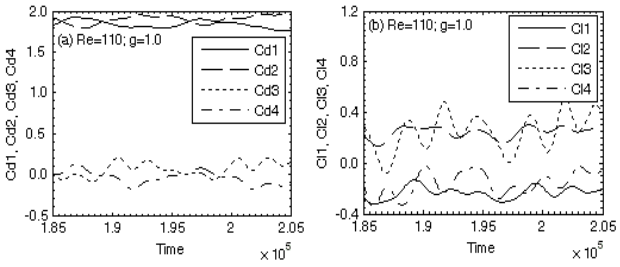

Fig. 10. Time analysis of drag and lift coefficients.

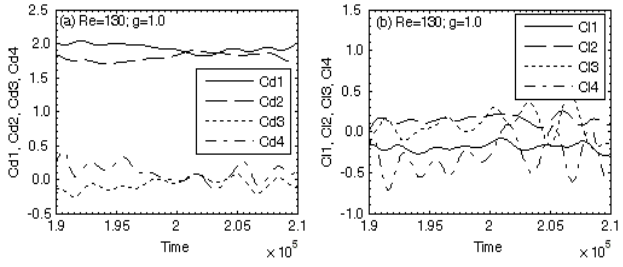

Fig. 11. Time signal analysis of drag and lift coefficients.

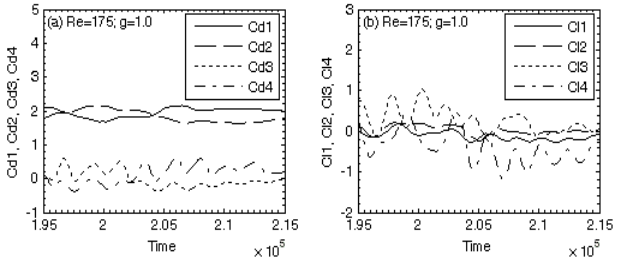

Fig. 12. Time history analysis of drag and lift coefficients.

At g=3.0, the time signal analysis of drag (cd1, cd2, cd3, cd4) and lift (cl1, cl2, cl3, cl4) coefficients for Re=80, 110 and 150 are illustrated in Figs. 13 (a, b) – 15 (a, b). The time signal analysis of drag coefficients for upstream cylinders (c_1 and c_2) shows steady behavior for Re=80 and the downstream cylinders (c_3 and c_4) shows periodic behavior (see Fig. 13 (a, b)). Furthermore, the time signal analysis of lift coefficients (see Figs. 13 (a, b) – 15 (a, b)) shows the existence of only primary vortex shedding frequency. This ensures that the secondary cylinder interaction frequency almost disappears for all four cylinders. Furthermore, there exists some modulation in the drag coefficients. It is found that the time period of consecutive cycles is almost same. The in-phase and anti-phase wiggling shielding wake patterns clearly seen from the time signal analysis of lift coefficients.

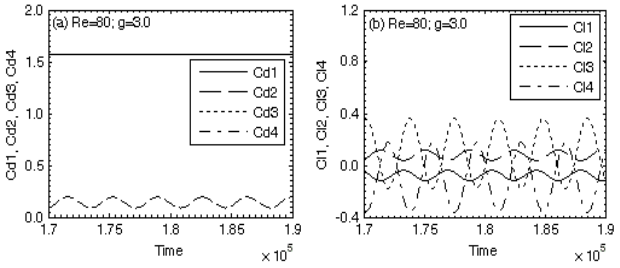

Fig. 13. Time analysis of drag and lift coefficients.

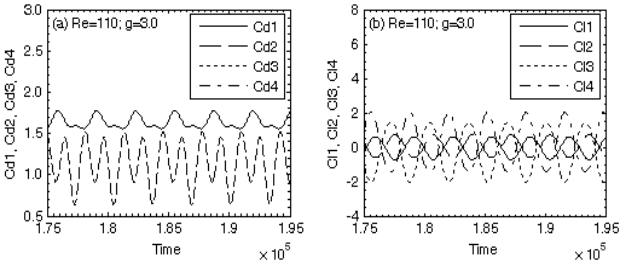

Fig. 14. Time signal analysis of drag and lift coefficients.

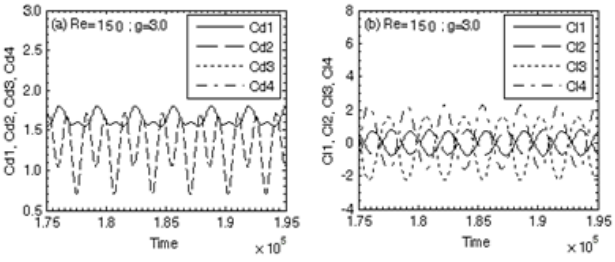

Fig. 15. Time history analysis of drag and lift coefficients.

The in-phase and anti-phase vortex shedding wake pattern clearly seen from the time signal analysis of drag and lift coefficients (see Figs. 16 and 17 (a, b)). The sinusoidal natures for both drag and lift coefficients observed. It is found that the oscillation frequency of the drag coefficient is almost double than the lift coefficient oscillation frequency for all four cylinders. It is examined that the temporal variation of lift coefficients between the upstream and downstream cylinders are close to zero degree or 180 degree. The present investigation is in agreement with the numerical findings of Chatterjee *et al.* [24] for flow past row of square cylinders using the lattice Boltzmann method for g=4.0 and Re=150.

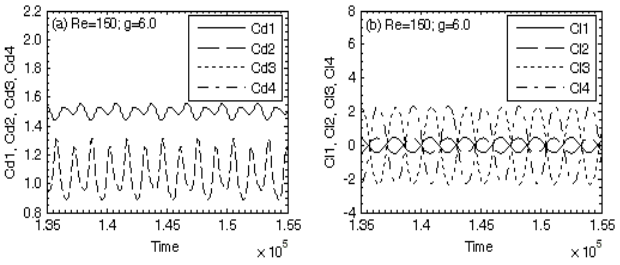

Fig. 16. Time analysis of drag and lift coefficients.

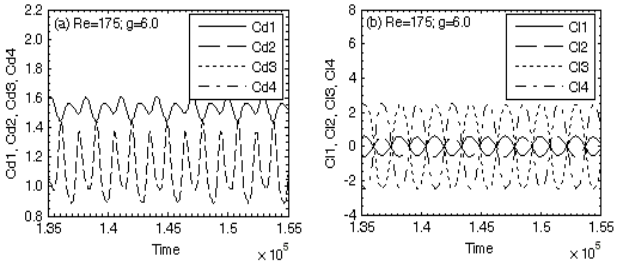

Fig. 17. Time signal analysis of drag and lift coefficients.

3.3 Vortex shedding frequency

It is important to state here that for Re=60, 80 and 90 at g=1.0 not observed any primary and secondary cylinder interaction frequency for four cylinders in this study. The power spectrum analysis of lift coefficients for Re= 130 and 175 at g=1.0 in Figs. 18-19(a, d) clearly shows the existence of broad and continuous spectrum, characteristics of stable shielding wake pattern. The power spectrum analysis clearly indicates the presence of secondary cylinder interaction frequencies for all four cylinders at g=1.0. The time signal analysis of lift coefficients for Re=130 (see Figs. 18 (a-d)) clearly indicates the presence of secondary cylinder interaction frequencies. The highest peak in Fig. 18 (a-d) (St=0.0936, 0.1410, 0.1346 and 0.1410 for upstream (c_1 and c_2) and downstream (c_3 and c_4) cylinders) and in Fig. 19(a-d) (St=0.0343, 0.0348, 0.1631 and 0.0239 for upstream and downstream cylinders) is the primary vortex shedding frequency. Furthermore, the multi peaks represent the secondary cylinder interaction frequencies. Kumar *et al.* [23] for flow past row of square cylinders for the first time proposed the secondary cylinder interaction frequency concept.

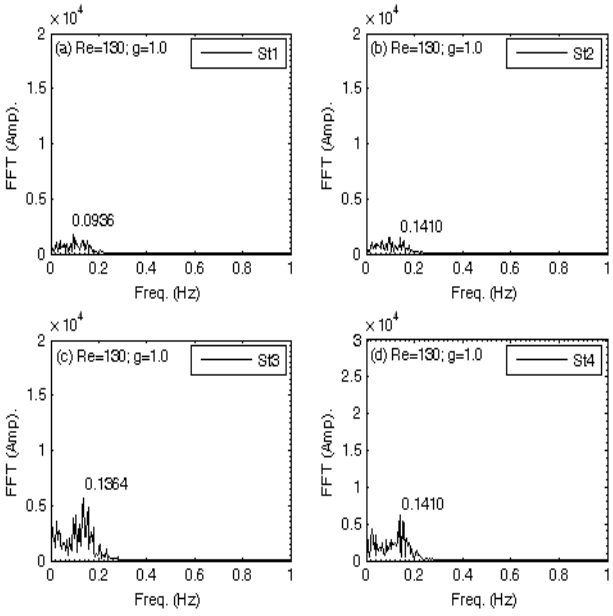

Fig. 18. Power spectrum analysis for lift coefficients for Re = 130 and g=1.0.

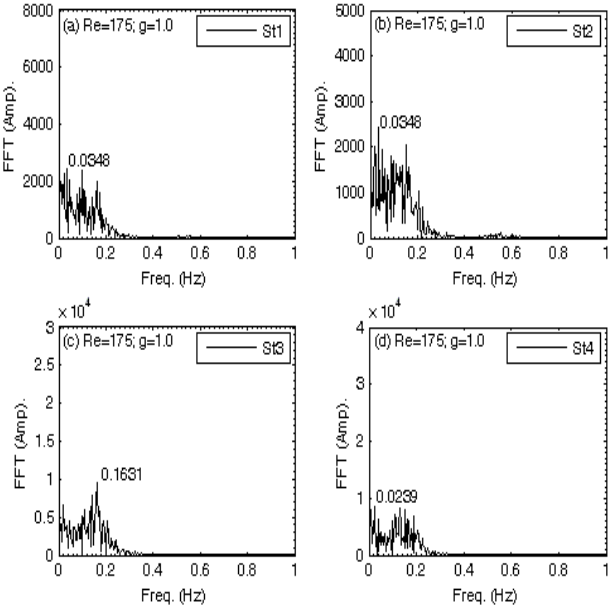

Fig. 19. Power spectrum analysis for lift coefficients for Re = 175 and g=1.0.

The power spectrum analysis for g=3.0 for two chosen Reynolds numbers (Re=80 and 120) for all four square cylinders are shown in Figs. 20-21 (a-d). It is found that there exists only primary vortex shedding frequency at intermediate gap spacing. A Strouhal number of 0.1203, 0.1243, 0.1203 and 0.1243 corresponds to the primary vortex shedding frequency for c_1, c_2, c_3 and c_4 at Re=80, respectively. Similarly, 0.1417, 0.1410, 0.1417 and 0.1410 corresponds to Strouhal number for c_1, c_2, c_3 and

c_4 at Re=120, respectively. It is found that there exists one small peak for downstream cylinders (c_3 and c_4) in Figs. 20 (c, d) and 21 (c, d). The same characteristics observed for all chosen Reynolds numbers at g=3.0 in this study (not shown). The oscillation frequency of lift coefficients for four cylinders is almost same for all Reynolds numbers. This ensures that there is no secondary cylinder interaction frequency for wiggling shielding wake pattern. Chatterjee *et al.* [24] observed similar characteristics for flow past row of square cylinders.

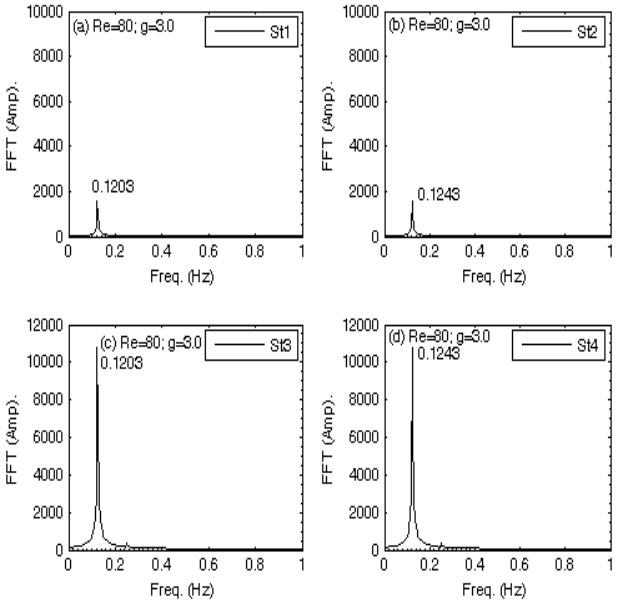

Fig. 20. Power spectrum analysis for lift coefficients for Re = 80 and g=3.0.

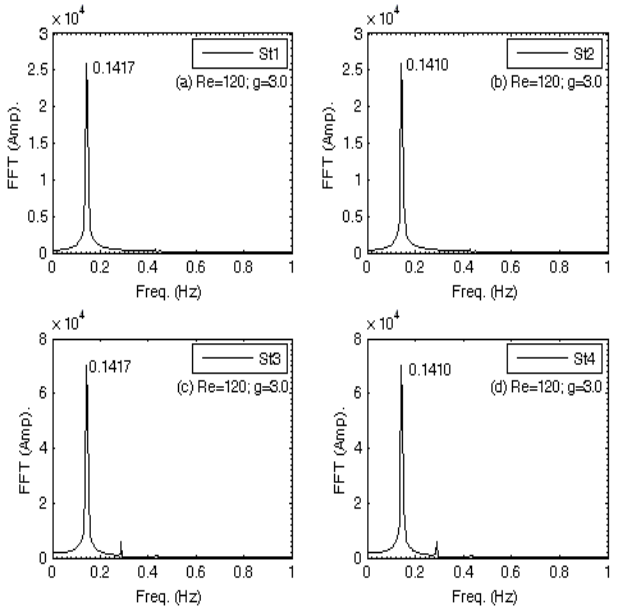

Fig. 21. Power spectrum analysis for lift coefficients for Re = 120 and g=3.0.

At g=6.0, the wake pattern not affected by the secondary cylinder interaction frequency and the primary vortex shedding frequency fully dominated the vortex shedding wake pattern (see Figs. 22-23 (a-d)). Some representative cases such as Re=90 (Fig. 22 (a-d)) and Re=175 (Fig. 23 (a-d)) are presented in this sub-section. The lift coefficients spectrum analysis shows similar characteristics for other Reynolds number (not shown) in this study.

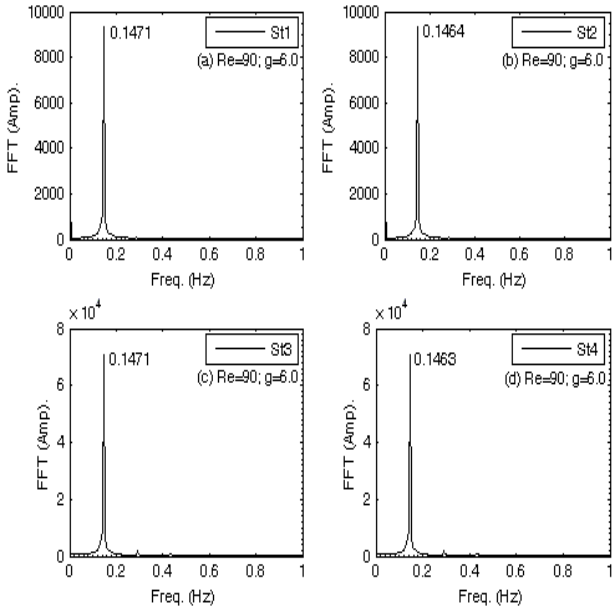

Fig. 22. Power spectrum analysis for lift coefficients for Re = 90 and g=6.0.

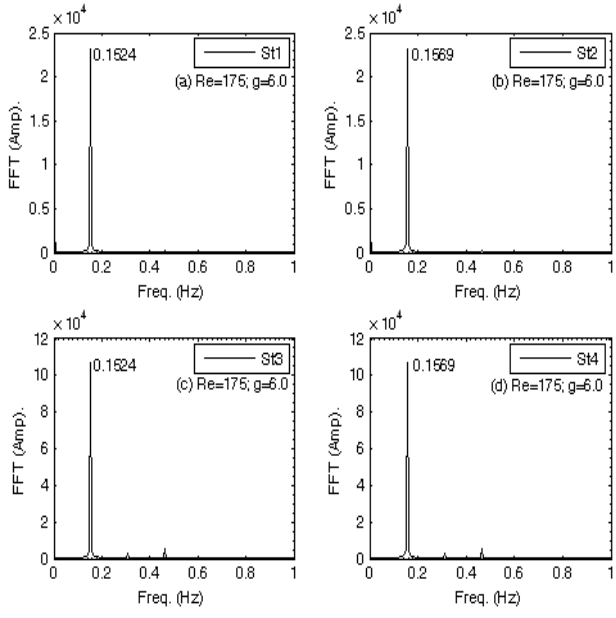

Fig. 23. Power spectrum analysis for lift coefficients for Re = 175 and g=6.0.

3.4 Statistical analysis

The variation of physical parameters such as Cdmean, St, Cdrms and Clrms with gap spacing (g= 1.0, 3.0 and 6.0) at different Reynolds number is shown in Figs. 24-26 (a-d). At g=3.0 and 6.0, the Cdmean, Cdrms and Clrms of upstream cylinders (c_1 and c_2) and downstream cylinders (c_3 and c_4) are almost same or close to each other. Thus, in this section we mainly discuss cylinders c_1 and c_4. Lam *et al.* [17] examined similar characteristics for four circular cylinders numerically. It is found that the Cdmean is either slightly increases or decreases with a increase in Reynolds number for all four cylinders (see Fig. 24 (a)). The present results show that at g=1.0 and Re=130 that the Cdmean value of cylinder (c_3) is negative. Similarly we observed the negative value for cylinder (c_4) at g=1.0 and Re=110 (see Fig. 24(a)). Sayers [7] and Lam and Fang [10] also observed the negative values for fourth cylinder at g≤2.0. They not observed the negative value for the third cylinder. This means that the free shear layers from first and second cylinders, after shielding behind third and fourth cylinders induce a strong backflow that produce a negative drag. Compared to upstream cylinders the downstream cylinders gives quite different values for third and fourth cylinders. The upstream cylinders shows higher values compared to single isolated cylinder and the downstream cylinders values are lower than isolated cylinder value. We not observed Strouhal number for Re=60, 80 and 90 in this study. For other Reynolds number the Strouhal number value for all four cylinders lower than the single cylinder value (see Fig. 24(b)). The Cdrms value of four cylinders shows an increasing behavior for various Reynolds number and higher than the single cylinder value (see Fig. 24(c)). Furthermore, for some Reynolds number (Re=150, 160 and 175) the upstream cylinders shows higher value than single cylinder value (see Fig. 24(d)). It is found that Clrms values of all cylinders are lower than the isolated cylinder value. These characteristics clearly tell us that there is strong interaction of wakes behind the downstream cylinders and no vortices generated between the upstream and downstream cylinders.

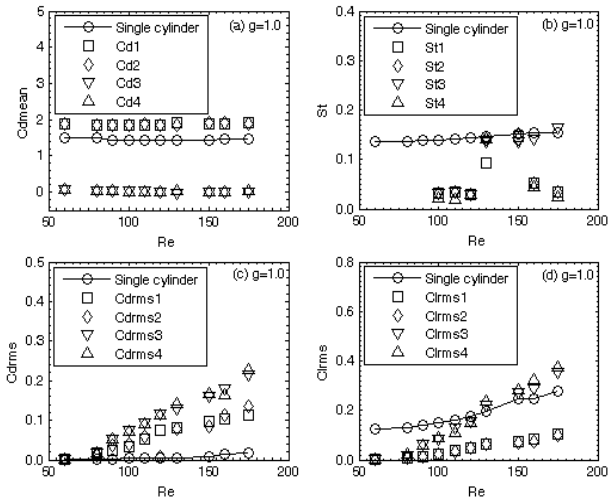

Fig. 24. Variation of engineering parameters for various Reynolds numbers at g = 1.0.

The mean drag coefficient value for upstream and downstream cylinders is almost equal. It is found that the upstream cylinders (c_1 and c_2) values are close to isolated cylinder. On the other hand, the downstream cylinders (c_3 and c_4) shows a jump between Re=100 and 110 for Cdmean (see Fig. 25(a)). This jump clearly shows when the in-phase wiggling shielding wake pattern (Re=100) change to anti-phase wiggling shielding wake pattern (Re=110). The Strouhal number parameter is not affected too much (see Fig. 25(b)). Furthermore, the Cdrms and Clrms for upstream cylinders are close to isolated cylinder and the downstream cylinders increases with the increase of Reynolds number (see Fig. 25(c, d)).

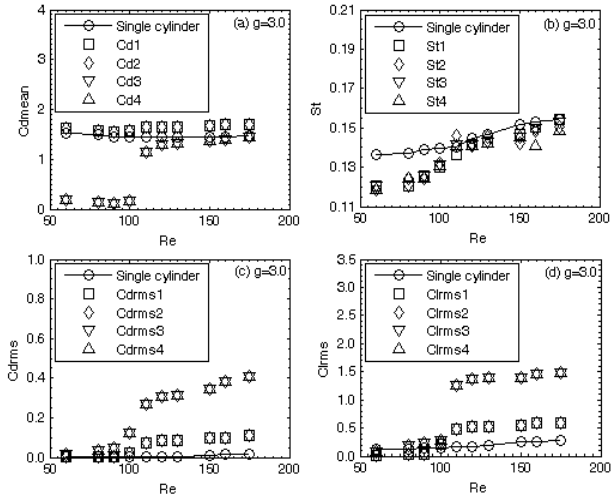

Fig. 25. Variation of engineering parameters for different Reynolds numbers at g = 3.0.

In order to further confirm the wake interaction mechanism and explanation discussed in section 3, the statisti-

cal data for large gap spacing presented in Figs. 26(a-d). This data ensures that the adjoining wakes isolated practically, and the interaction between the four cylinders wakes almost negligible. At relatively large gap spacing the physical parameters not affected too much (see Fig. 26(a-d)). It is found that for all engineering parameters the upstream cylinders (c_1 and c_2) values are almost close to single isolated cylinder value. Furthermore, the Cdmean value of downstream cylinders (c_3 and c_4) are lower than the isolated value and the other parameters such as St, Cdrms and Clrms values are higher than the isolated cylinder. The observed wake patterns in this study for different Reynolds number shown in Table 3.

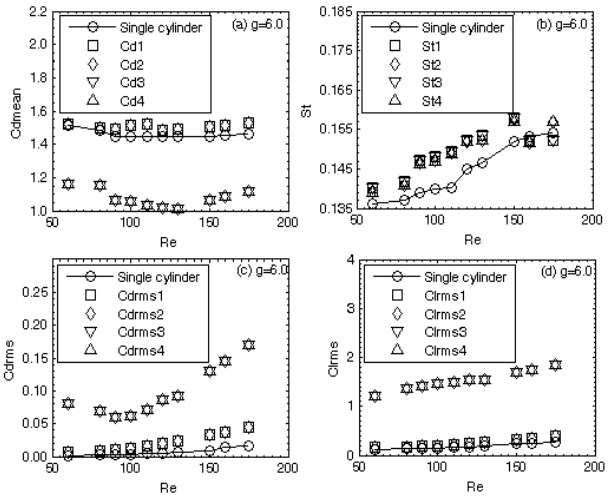

Fig. 26. Variation of engineering parameters for various Reynolds numbers at g = 6.0.

Table. 3. Wake patterns against Reynolds number.

g	Re	Wake Pattern
1.0	60	Steady
1.0	80≤Re≤175	Stable shielding
3.0	60, 80, 90, 100, 130, 150	In-phase wiggling shielding
3.0	110, 120, 160, 175	Anti-phase wiggling shielding
6.0	120, 150, 160	In-phase vortex shedding
6.0	60, 80, 90, 100, 110, 130, 175	Anti-phase vortex shedding

4. Conclusion

The numerical results of two-dimensional flow past four square cylinders in an in-line square configuration for gap spacing are reported in this present numerical study. The main agenda of the present work is to fully understand the effect of Reynolds number on steady, stable shielding, wiggling shielding (in-phase and anti-phase) and vortex shedding (in-phase and anti-phase) wake patterns. Furthermore, we study the effects of secondary cylinder interaction frequency in the time history analysis of drag and lift coefficients and power spectrum analysis of lift coefficient. Important findings are given below:

(i) At g = 1.0 substantial effect of Reynolds number is found. At g = 3.0 and 6.0 and larger Reynolds numbers the primary vortex shedding frequency dominates the flow and the secondary cylinder interaction frequency disappears. This means that at intermediate and relatively large gap spacing there is a week interaction of wakes behind the four cylinders, especially, with an increase in the Reynolds number. For g = 1.0 for all Reynolds numbers observed strong wakes interaction and compared to primary vortex shedding frequency the secondary cylinder interaction frequency predominates the flow.

(ii) The wake interaction mechanism in this paper is viewed from a shedding frequency perspective. At larger unequal gap spacing g = 3.0 and 6.0, the interaction between the wakes is too weak and observed between the cylinders continuous jet flow. On the other hand, at smaller unequal gap spacing g = 1.0 the interaction of wakes strongly depends on the Reynolds number. It is argued that the interaction of wakes occurs due to jet flow between the cylinders. The gap spacing is responsible for the lateral movement of different jets. In stable shielding wake pattern the jets strongly spread laterally due to small gap spacing. As a result of such strong jets spread the generated wakes are just behind the four cylinders broken immediately and the produce jets quickly merge together. Thus, at smaller gap spacing the secondary cylinder interaction frequency strongly affects the primary vortex shedding frequency.

(iii) In this work we observed that the widening and narrowing of wakes is the main cause of secondary cylinder interaction frequency which strongly affects the primary vortex shedding frequency as a result of gap spacing and increasing the Reynolds number. The proposed mechanism clearly tells us when the shed vortices move independently and when the merging of the jets strongly affect the wake interaction between the cylinders for unequal gap spacing. Specifically, in this study for unequal gap spacing and Reynolds number affect the wake interaction mechanism clearly and systematically brought out more insight and fruitful informations which observed experimentally in several studies.

(iv) We found that at g=1.0 and Re=130 the Cdmean value of cylinder (c_3) is negative. Similarly we observed the negative value for cylinder (c_4) at g=1.0 and Re=110. This means that the free shear layers from first and second cylinders, after shielding behind third and fourth cylinders induce a strong backflow that produce a negative drag.

Nomenclature

c_1 : First square cylinder

c_2 : Second square cylinder

c_3 : Third square cylinder
c_4 : Fourth square cylinder
C_s : Speed of sound
Cd : Drag coefficients
Cl : Lift coefficients
Cdmean : Mean drag coefficients
Cdmean1 : First cylinder mean drag coefficients
Cdmean2 : Second cylinder mean drag coefficients
Cdmean3 : Third cylinder mean drag coefficients
Cdmean4 : Fourth cylinder mean drag coefficients
C_{drms} : Root-mean-square value of drag coefficients
C_{lrms} : Root-mean-square value of lift coefficients
d : Diameter of the three cylinders
D : Dimensions
$\boldsymbol{e}_i$: Direction of the velocity
FD : Force components in in-line directions
FL : Force components in transverse directions
f_s : Vortex shedding frequency
g_i : Particle distribution function
$g_i^{(eq)}$: Equilibrium distribution function
g : Gap spacing between three cylinders
H : Height of the computational domain
L_1 : Upstream location
L_2 : Downstream location
n : Number of particles
p : Pressure
Re : Reynolds numbers
St : Strouhal number
St1 : First cylinder Strouhal number
St2 : Second cylinder Strouhal number
St3 : Third cylinder Strouhal number
St4 : Fourth cylinder Strouhal number
s : Surface-to-surface distance between cylinders
t : Dimensionless time
$\boldsymbol{u}$: Flow velocity
U_∞ : Uniform inflow velocity
w_i : Weighting functions
$\boldsymbol{x}$: Position of the particle
ρ : Fluid density
τ : Single-relaxation time parameter
υ : Kinematic viscosity

References

[1] D. Sumner, S. S. T. Wong, S. J. Price and M. P. Paidoussis, Fluid behavior of side-by-side circular cylinders in steady cross-flow, *J. Fluids Struct*. 13 (3) (1999) 309-338.

[2] D. W. Guillaume and J. C. LaRue, Investigation of the flopping regime with, -three- and four-cylinder arrays, *Exp. Fluids* 27 (2) (1999) 145-156.

[3] S. Kang, Characteristics of flow over two circular cylinders in a side-by-side arrangement at low Reynolds numbers. *Phys. Fluids*. 15 (9) (2003) 2486-2498.

[4] A. Agrawal, L. Djenidi and R. A. Antonia, Investigation of flow around a pair of side-by-side square cylinders using the lattice Boltzmann method, *Comp. Fluids*. 35 (10) (2006) 1093-1107.

[5] M. M. Zdravkovich, The effect of interference between circular cylinders in cross flow, *J Fluids Struct*. 1 (1987) 239-261.

[6] M. M. Alam, Y. Zhou and X. W. Wang, The wake of two side-by-side square cylinders, *J. Fluid Mech*. 669 (2011) 432-471.

[7] A. T. Sayers, Flow interference between four equispaced cylinders when subjected to a cross flow, *J. Wind Eng. Ind. Aero*. 31 (1988) 9-28.

[8] A. T. Sayers, Vortex shedding from groups of three and four equispaced cylinders situated in cross-flow, *J. Wind Eng. Ind. Aero*. 34 (1990) 213-221.

[9] K. Lam and S. C. Lo, A visualization study of cross-flow around four cylinders in a square configuration, *J. Fluids Struc*. 6 (1992) 109-131.

[10] K. Lam and X. Fang, The effect of interference of four equispaced cylinders in cross flow on pressure and force coefficients, *J. Fluids Struc*. 9 (1995) 195-214.

[11] K. Lam, J. Y. Li, K. T. Chen and R. M. C. So, Velocity amp and flow pattern of flow around four cylinders in a square configuration at low Reynolds number and large spacing ratio using particle image velocimetry, In: *Proc. Of the second Int. Conf. on Vortex Methods, Istanbul, Turkey*. (2001b).

[12] K. Lam, J. Y. Li, K. T. Chen and R. M. C. So, The flow patterns of cross flow around four cylinders in an in-line square configuration. In: *The Tenth Int. Symp. On flow Vis. Kyoto, Japan.* (2002).

[13] K. Lam, J. Y. Li, K. T. Chen and R. M. C. So, Flow pattern and velocity field distribution of cross-flow around four cylinders in a square configuration at low Reynolds number, *J. Fluids Struc*. 17 (2003a) 665-679.

[14] K. Lam, J. Y. Li. and R. M. C. So, Force coefficient and Strouhal numbers of four cylinders in cross flow, *J. Fluids Struc*. 18 (2003b) 305-324.

[15] T. Farrant, M. Tan, and W. G. Price, A cell boundary element method applied to laminar vortex-shedding from arrays of cylinders in various arrangements, *J. Fluids Struc*. 14 (2000) 375-402.

[16] K. Lam, R. M. C. So and J. Y. Li, Flow around four cylinders in a square configuration using surface vorticity method. In: *Proc. Of the Second Int. Conf. on Vortex Methods, Istanbul, Turkey*, (2001a).

[17] K. Lam, W. Q. Gong and R. M. C. So, Numerical simulation of cross-flow around four cylinders in an in-line square configuration, *J. Fluids Struc*. 24(2008) 34-57.

[18] K. Lam and L. Zou, Experimental and numerical study for the cross-flow around four cylinders in an in-line square configuration, *J. Mech. Sci. Tech*. 21 (2007) 1338-1343.

[19] A. Dutta, P. Goyal, R. K. Singh and K. K. Vaze, Fluid flow analysis for cross-flow around four cylinders arranged in a square configuration, *Excerpt from the Proc. Of the COMSOL Conf. India*, (2010).

[20] K. Lam and L. Zou, Three-dimensional numerical simula-

tions of cross-flow around four cylinders in an in-line square configuration, *J. Fluids Struc*. 26 (2010) 482-502.
[21] S. Ul. Islam, C. Y. Zhou and F. Ahmad, Numerical simulations of cross-flow around four square cylinders in an in-line rectangular configuration, *World Acad Sci, Engg Tech*. 33 (2009) 824-833.
[22] J. Mizushima and T. Akinaga, Vortex shedding from a row of square bars, Fluid Dyn Res. 32 (2003) 179-191.
[23] S. R. Kumar, A. Sharma and A. Agarwal, Simulation of flow around a row of square cylinders, *J. Fluid Mech*. 606 (2008) 369-392.
[24] D. Chatterjee, G. Biswas and S. Amiroudine, Numerical simulation of flow past row of square cylinders for various separation ratios, *Comp. Fluids*. 39 (2010) 49-59.
[25] C. H. K. Williamson, Evolution of a single wake behind a pair of bluff bodies, *J. Fluid Mech.* 159 (1985) 1-18.
[26] S. Chen and G. Doolen, Lattice Boltzmann method for fluid flows, *Ann Rev Fluid Mech*. 30 (1998) 329-364.
[27] A. A. Mohamad, Lattice Boltzmann Method: Fundamentals and Engineering Applications with Computer Codes, Springer-Verlag London Limited (2011).
[28] S. Succi, Lattice Boltzmann Method for fluid dynamics and beyond. Oxford, UK: Oxford Univ. Press; 2001.
[29] U. Frisch, B. Hasslacher and Y. Pomeau, Lattice gas automata for the Navier-Stokes equations, *Phys Rev Lett*. 56 (1986) 1505-1508.
[30] M. Breuer, J. Bernsdorf, T. Zeiser and F. Durst, Accurate computations of the laminar flow past a square cylinder based on two different methods: lattice-Boltzmann and finite-volume, *Int J Heat Fluid Flow*. 21 (2000) 186-196.
[31] A. J. C. Ladd and R. Verberg, Lattice Boltzmann simulations of particle-fluid suspensions, *J. Stat. Phys*. 104 (2001) 1191-1251.
[32] M. C. Sukop and D. T. Thorne, Lattice Boltzmann Modeling: an Introduction for Geoscientists and Engineers. Springer-Verlag Berlin/Heidelberg, (2006).
[33] A. Okajima, Strouhal numbers of rectangular cylinders, *J. Fluid Mech*. 123 (1982) 379-398.
[34] R. W. Davis and E. F. Moore, A numerical study of vortex shedding from rectangles, *J. Fluid Mech*. 116(1982) 475-506.
[35] S. Dutta, P. K. Panigrahi and K. Muralidhar, Effect of orientation on the wake of a square cylinder at low Reynolds numbers, *Ind. J. Eng. Mat. Sci*. 11 (2004) 447-459.
[36] B. Gera, P. K. Sharma and R. K. Singh, CFD analysis of 2D unsteady flow around a square cylinder, *Int. J. App. Engg. Res. Din*. 1 (3) (2010) 602-610.
[37] S. Malekzadeh and A. Sohankar, Reduction of fluid forces and heat transfer on a square cylinder in a laminar flow regime using a control plate, *Int. J. Heat Fluid Flow*. 34 (2012) 15-27.

Shams Ul Islam is currently an assistant professor in Mathematics Department, COMSATS Institute of Information Technology, Islamabad, Pakistan. He received his PhD in 2010. His research interests include fluid structure interaction, numerical investigation of bluff body flows, heat and mass transfer.

Suvash C. Saha is currently a Postdoctoral Fellow in the School of Chemistry, Physics and Mechanical Engineering, Queensland University of Technology, Brisbane, Australia. He obtained his PhD from James Cook University in 2009. His research interests include deformation of RBC's, mesh free method, heat and mass transfer.